Supplementary material for: *Is the subtropical jet shifting poleward?*

Penelope Maher · Michael E. Kelleher · Philip Sansom · John Methven

Penelope Maher, Michael E. Kelleher and Philip Sansom
Department of Mathematics, University of Exeter, Exeter, UK. E-mail: p.maher@exeter.ac.uk

John Methven
Department of Meteorology, University of Reading, Reading, United Kingdom.

Present address: of M. E. Kelleher Climate Change Science Institute, Oak Ridge National Laboratory, Oak Ridge, TN, USA

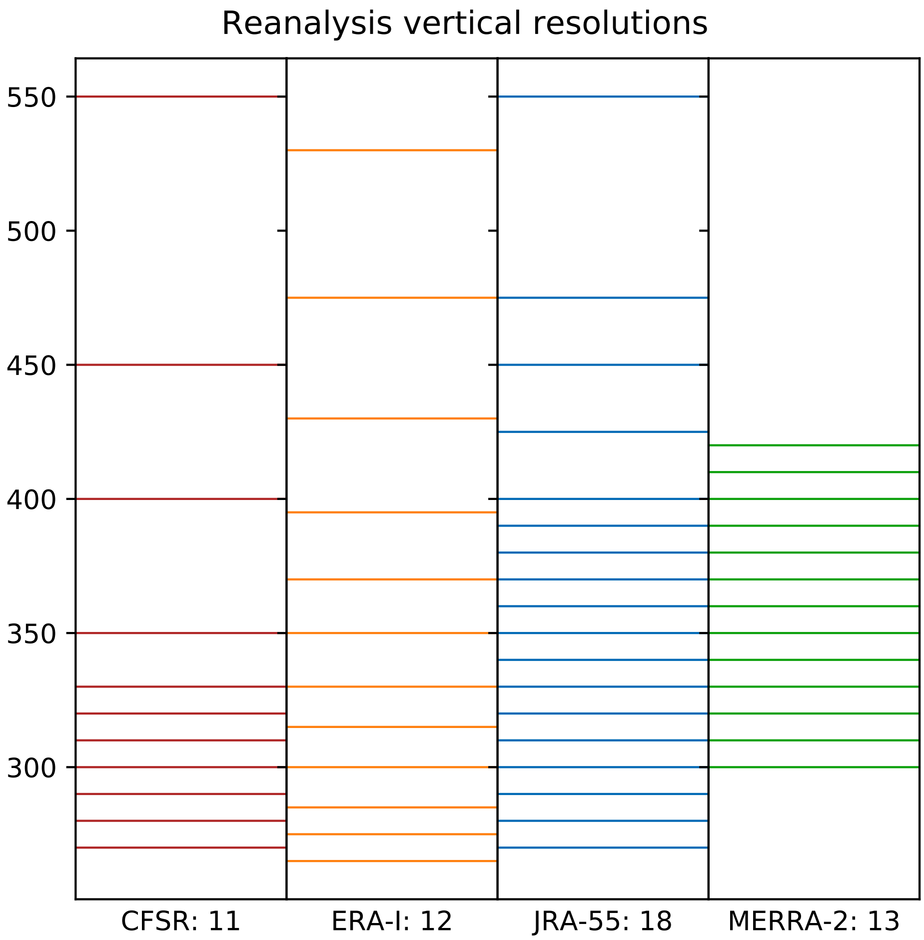

Fig. S1 The vertical resolution (in θ (K)) of each reanalysis product. The x-axis labels indicate the reanalysis and total number of vertical levels.

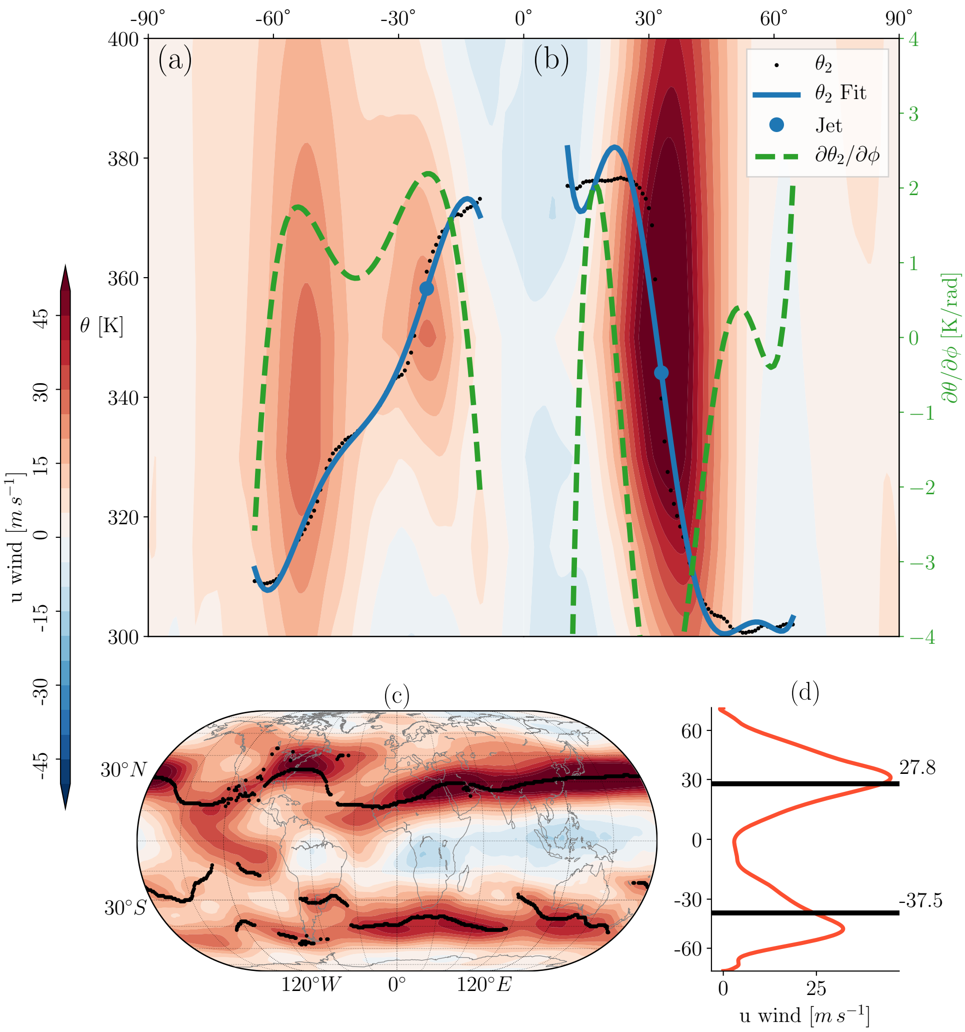

Fig. S2 As in Fig. 2 but for January 2013, $\phi_{NH} = 30.0°$ N and $\phi_{SH} = 37.5°$ S

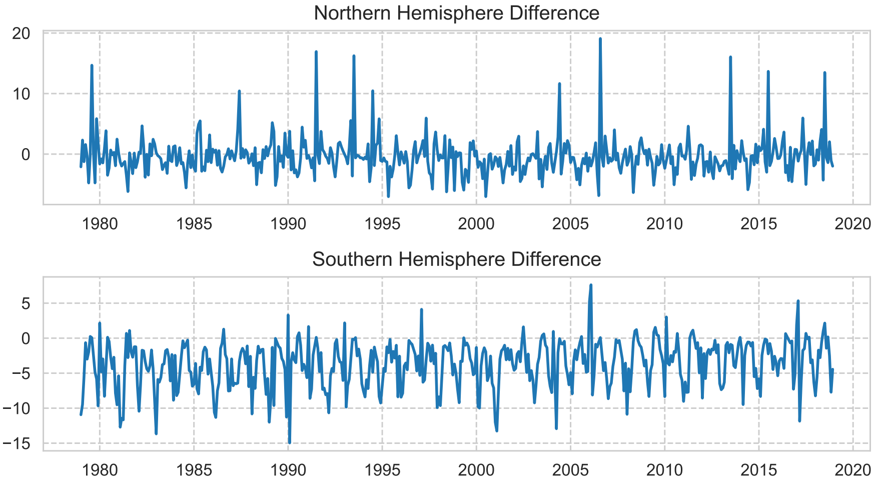

Fig. S3 As in Fig. 3 but for the tropopause gradient time series minus the Davis and Birner [2016] time series. Positive NH and negative SH values correspond to the tropopause gradient method that is further poleward than the Davis and Birner [2016] method.

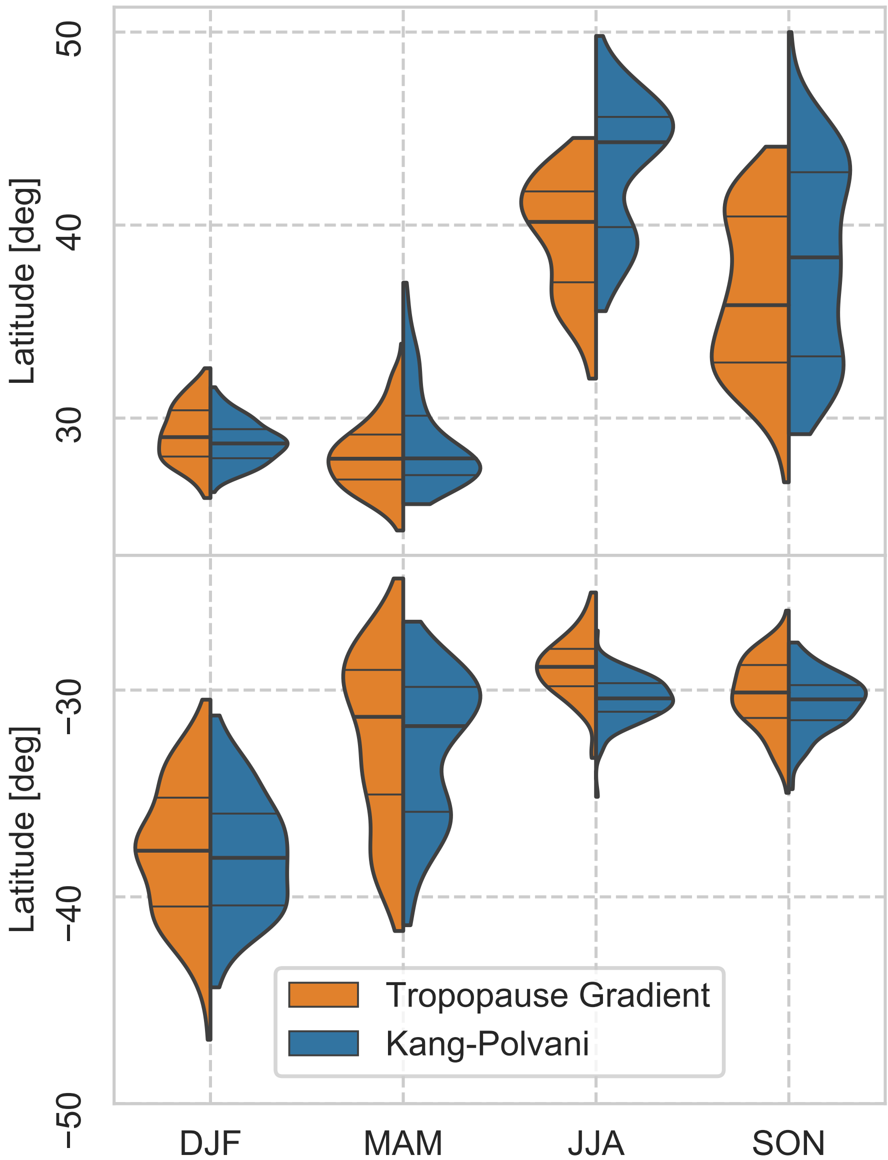

Fig. S4 As in Fig. 4 but for the adapted Kang and Polvani [2011] method.

Sensitivity to Parameters

Table S1 The linear sensitivities of seasonal mean jet latitude to the PV level, degree of polynomial fit, and the min and max latitudes. Where bold, the sensitivity is statistically different from 0 at $\alpha = 0.05$. The values correspond to the slopes of Fig. S5-S8

	PV Lev		Deg Fit		Min ϕ		Max ϕ	
	NH	SH	NH	SH	NH	SH	NH	SH
DJF	**2.27**	**-2.48**	-2.17	-0.46	**-0.22**	0.03	**0.02**	-0.02
MAM	**2.24**	**-2.42**	-2.78	-0.70	**-0.33**	0.00	**0.07**	0.03
JJA	**2.13**	**-1.98**	-1.04	**-0.83**	-0.04	**0.13**	**0.14**	**0.05**
SON	**2.77**	**-2.16**	-1.45	**-0.88**	**-0.15**	**0.05**	**0.06**	**0.06**

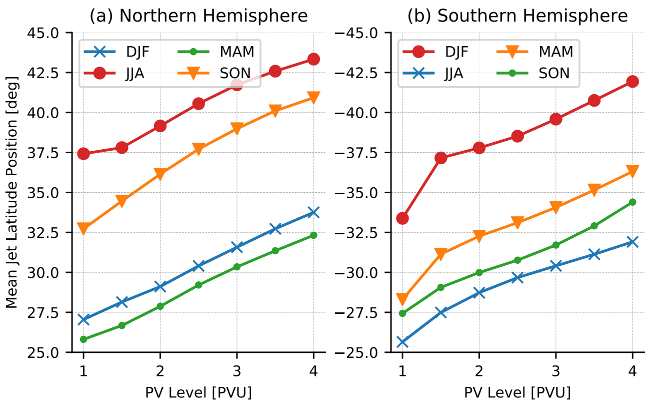

Fig. S5 Sensitivity of seasonal mean jet position to the PV level using ERA-I monthly data (a) NH in boreal winter (blue x), summer (red large circles), spring (green small circles), and autumn (orange triangles), (b) SH for equivalent austral seasons with the same color and marker. See Table S1 for the significance of the linear slopes.

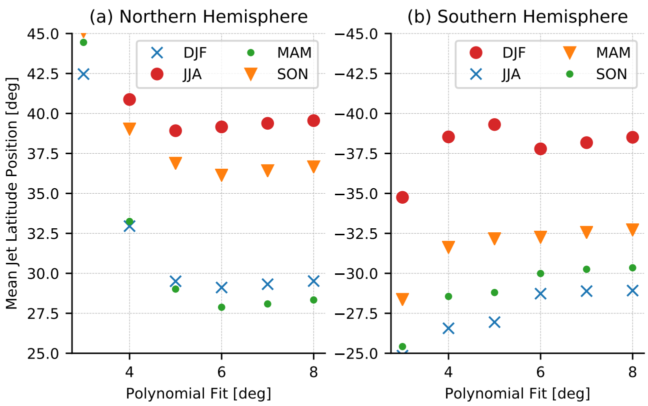

Fig. S6 As in Fig. S5 but for sensitivity to the degree of polynomial fit. See Table S1 for the significance of the linear slopes.

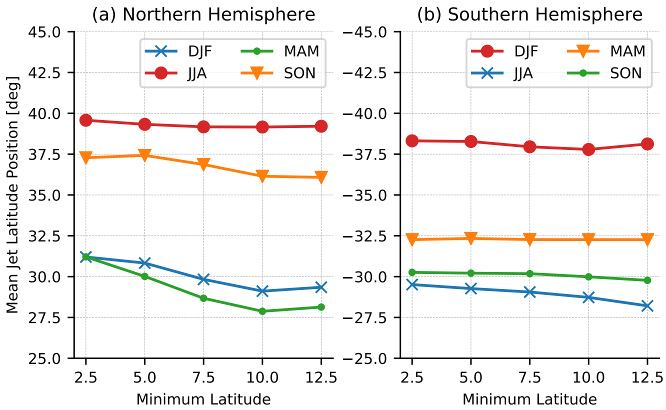

Fig. S7 As in Fig. S6 but for sensitivity to the minimum latitude threshold. See Table S1 for the significance of the linear slopes.

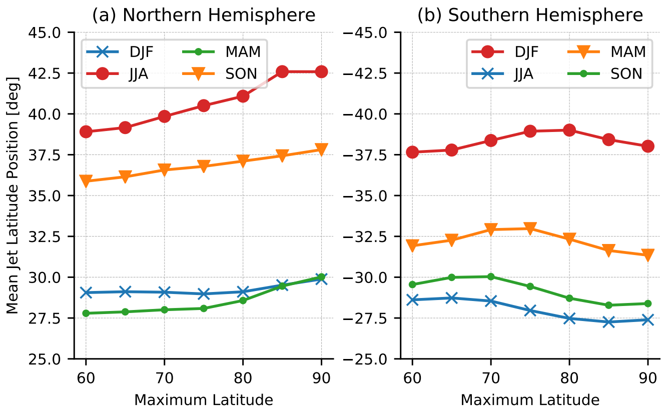

Fig. S8 As in Fig. S6 but for sensitivity to the maximum latitude threshold. See Table S1 for the significance of the linear slopes.

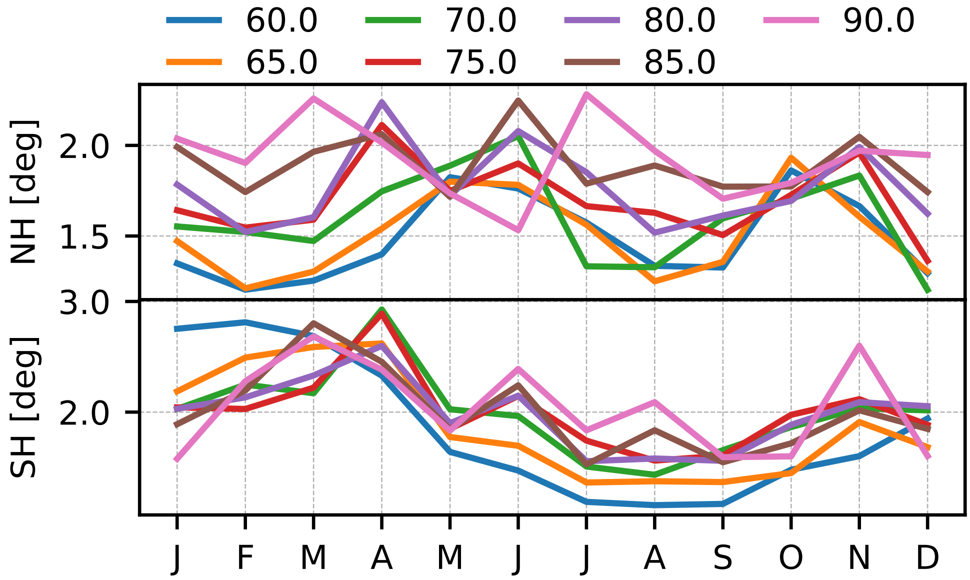

Fig. S9 Monthly interannual standard deviation of the subtropical jet position for the (top) NH and (bottom) SH sensitivity to the maximum latitude threshold. Including a maximum threshold results in a more realistic annual cycle in the variability.

Subtropical Jet Properties

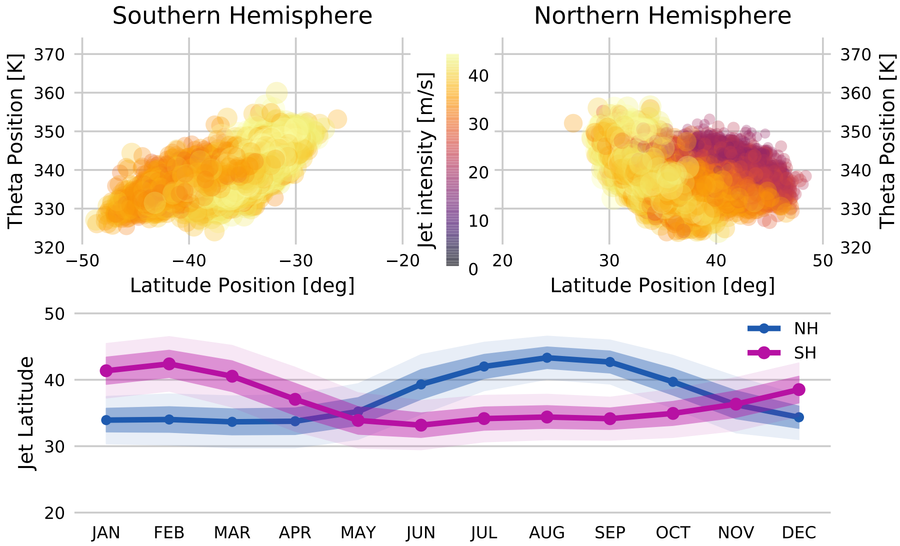

Fig. S10 As in Fig. 4 but for daily data. See Table S5 for daily subtropical jet values.

Table S2 Annual and seasonal mean values of the subtropical jet latitude, intensity and height (measured in θ) for **monthly CFSR/CFSv2** data.

	$\phi[°]$		Int $[ms^{-1}]$		θ[K]	
	SH	NH	SH	NH	SH	NH
Annual	-32.5	33.4	31.8	30.5	341.1	342.0
DJF	-37.4	30.4	28.2	41.5	337.0	342.0
JJA	-29.9	38.6	37.0	20.1	342.7	341.1
MAM	-31.8	28.4	29.4	31.8	342.9	346.8
SON	-30.8	36.4	32.4	28.7	342.0	338.2

Table S3 As in S2 but for **daily CFSR/CFSv2** data.

	$\phi[°]$		Int $[ms^{-1}]$		θ[K]	
	SH	NH	SH	NH	SH	NH
Annual	-35.2	36.5	39.1	35.6	340.1	340.3
DJF	-39.3	32.7	35.4	45.8	336.7	341.2
JJA	-32.3	41.1	44.2	24.9	342.7	340.3
MAM	-35.4	33.3	37.2	37.4	340.4	342.3
SON	-33.7	38.8	39.6	34.5	340.6	337.5

Table S4 As in S2 but for **monthly ERA-I** data.

	$\phi[°]$		Int $[ms^{-1}]$		θ[K]	
	SH	NH	SH	NH	SH	NH
Annual	-32.3	33.3	33.0	30.5	342.0	343.1
DJF	-37.8	29.2	29.0	41.9	337.5	344.1
JJA	-28.9	39.5	38.8	19.1	344.0	341.4
MAM	-32.4	28.1	30.9	32.1	343.1	348.0
SON	-30.2	36.4	33.5	28.9	343.4	339.0

Table S5 As in S2 but for **daily ERA-I** data.

	$\phi[°]$		Int $[ms^{-1}]$		θ[K]	
	SH	NH	SH	NH	SH	NH
Annual	-36.7	37.4	38.9	32.6	338.3	339.3
DJF	-40.7	34.1	35.1	41.8	336.1	338.0
JJA	-33.9	41.6	43.1	21.5	339.4	341.3
MAM	-37.2	34.2	37.6	34.7	338.7	340.9
SON	-35.1	39.5	39.7	32.7	338.7	336.8

Table S6 As in S2 but for **monthly JRA** data.

	$\phi[°]$		Int $[ms^{-1}]$		θ [K]	
	SH	NH	SH	NH	SH	NH
Annual	-30.0	31.3	33.0	31.4	347.1	346.3
DJF	-34.9	27.9	28.2	41.9	342.5	346.6
JJA	-27.8	37.3	39.4	20.7	348.1	343.8
MAM	-29.2	26.6	30.5	33.6	349.6	351.0
SON	-28.2	33.4	33.7	29.4	348.2	343.4

Table S7 As in S2 but for **daily JRA** data.

	$\phi[°]$		Int $[ms^{-1}]$		θ [K]	
	SH	NH	SH	NH	SH	NH
Annual	-35.3	36.8	38.0	33.4	341.4	340.3
DJF	-39.1	33.7	34.6	41.5	339.6	339.6
JJA	-33.1	41.4	41.8	23.6	341.7	341.0
MAM	-35.4	33.6	36.8	35.8	342.3	341.6
SON	-33.7	38.4	38.6	32.9	341.8	339.0

Table S8 As in Table S2 but for **monthly MERRA-2** data.

	$\phi[°]$		Int $[ms^{-1}]$		θ [K]	
	SH	NH	SH	NH	SH	NH
Annual	-29.7	31.4	30.8	31.6	353.5	352.3
DJF	-34.8	28.0	27.1	42.1	347.3	353.8
JJA	-27.6	37.1	37.0	21.4	356.3	350.0
MAM	-28.4	26.7	28.2	33.9	355.6	356.8
SON	-28.0	33.8	30.9	29.0	354.6	348.5

Table S9 As in Table S2 but for **daily MERRA-2** data.

	$\phi[°]$		Int $[ms^{-1}]$		θ [K]	
	SH	NH	SH	NH	SH	NH
Annual	-31.4	33.8	42.7	41.3	351.8	350.6
DJF	-35.8	29.4	37.3	51.5	346.6	354.1
JJA	-29.0	40.2	49.2	30.3	355.4	347.2
MAM	-31.3	29.6	41.1	45.4	352.4	354.3
SON	-29.7	35.8	43.0	38.4	352.9	347.0

Table S10 Decadal trends for each reanalysis product using the tropopause gradient method.

Data	Freq.	Trend [° dec^{-1}]	
		SH	NH
CFSR/CFSv2	monthly	**+0.70 (+0.49, +0.90)**	**-0.31 (-0.47, -0.14)**
ERA-I	monthly	**+0.37 (+0.19, +0.55)**	-0.08 (-0.22 , +0.07)
JRA55	monthly	+0.13 (-0.04, +0.30)	+0.11 (-0.05 , +0.26)
MERRA-2	monthly	+0.16 (-0.05, +0.37)	-0.05 (-0.19 , +0.08)
CFSR/CFSv2	daily	**+0.25 (+0.19, +0.31)**	**-0.08 (-0.13, -0.03)**
ERA-I	daily	-0.03 (-0.09, +0.03)	**+0.08 (+0.02, +0.14)**
JRA55	daily	**-0.10 (-0.16, -0.05)**	**+0.10 (+0.04, +0.16)**
MERRA-2	daily	+0.02 (-0.04, +0.09)	**+0.06 (+0.01, +0.12)**

Reliability of trend detection

In order to check whether we can reliably detect small trends, we performed a statistical power analysis as follows:

1. Fit the statistical model in equation 3 and obtain the maximum likelihood estimates of μ, a_1, b_1, a_2, b_2, α and σ^2.
2. Fix $\beta = \beta^\star$. For j in $1, \ldots, 1000$
   (a) Simulate a new time series ϕ_t^j of equal length from equation 3 given μ, $\beta^\star$, a_1, b_1, a_2, b_2, α and σ^2.
   (b) Re-fit the statistical model to the new data ϕ_t^j.
   (c) Test whether the estimate of $\beta^\star$ is significant at the 5 % level.

The percentage of samples j in which the test is significant for a particular value of the trend $\beta^\star$ is called the *power* of the test, and tells us how reliably we can detect trends of a particular size [Wilks, 2011, Chapter 5.1.5]. Power greater than around 0.8 is often used a threshold for a reliable test. By repeating this analysis for various trend sizes $\beta^\star$, we can build up a picture of the size of trend we can reliably detect, given the amount of data available.